Available online at www.sciencedirect.com
ScienceDirect
Journal of Natural Gas Chemistry 20(2011)611–617
Journal of Natural Gas Chemistry
www.elsevier.com/locate/jngc

A DFT theoretical study of CH_4 dissociation on gold-alloyed Ni(111) surface

Hongyan Liu[1,2], Ruixia Yan[1], Riguang Zhang[1], Baojun Wang[1*], Kechang Xie[1]

1. Key Laboratory of Coal Science and Technology of Ministry of Education and Shanxi Province, Taiyuan University of Technology, Taiyuan 030024, Shanxi, China; 2. College of Chemistry and Chemical Engineering, Shanxi Datong University, Datong 037009, Shanxi, China

[Manuscript received June 22, 2011; revised July 30, 2011]

Abstract

A density-functional theory (DFT) method has been conducted to systematically investigate the adsorption of CH_x ($x = 0\sim4$) as well as the dissociation of CH_x ($x = 1\sim4$) on (111) facets of gold-alloyed Ni surface. The results have been compared with those obtained on pure Ni(111) surface. It shows that the adsorption energies of CH_x ($x = 1\sim3$) are lower, and the reaction barriers of CH_4 dissociation are higher in the first and the fourth steps on gold-alloyed Ni(111) compared with those on pure Ni(111). In particular, the rate-determining step for CH_4 dissociation is considered as the first step of dehydrogenation on gold-alloyed Ni(111), while it is the fourth step of dehydrogenation on pure Ni(111). Furthermore, the activation barrier in rate-determining step is higher by 0.41 eV on gold-alloyed Ni(111) than that on pure Ni(111). From above results, it can be concluded that carbon is not easy to form on gold-alloyed Ni(111) compared with that on pure Ni(111).

Key words

adsorption; CH_4 dissociation; reaction barrier; *d*-band center

1. Introduction

Catalytic reforming of CH_4 with H_2O and CO_2 to produce synthesis gas has attracted increasing attention in recent years [1−7]. The conversion of the greenhouse gases into a valuable synthesis gas not only reduces emissions of greenhouse gas but also satisfies the requirement of many synthesis processes in chemical industry.

Ni-based catalysts, because of relatively low price and good initial reactivity as compared with noble metal, are selected to catalyze the reforming of CH_4. However, they are susceptible to deactivation from the deposition of carbon [8]. Carbon mainly results from CH_4 dissociation from thermodynamics viewpoint. In addition, isotopic studies and forward rate measurements confirmed the mechanistic equivalence among CH_4-reforming and decomposition of CH_4 on Ni-based catalysts [9]. Therefore, in order to understand carbon formation in detail, it is central to investigate CH_4 dissociation considered as a key and sole process.

In order to control the deactivation by carbon formation, modifying Ni catalysts with a second metal, such as gold, has been developed through alloy formation. Scanning tunneling microscopy (STM) study showed a change in geometry and electronic structure for gold-alloyed Ni catalyst, indicating that the chemical activity of Ni atoms may be modified by nearest-neighbor Au atoms [10]. Kratzer et al. [11,12] presented a DFT study of the first step of CH_4 dissociation on gold-alloyed Ni(111) surface, and found the reactivity of Ni atoms is affected by adjacent surface sites. However, the full mechanism of CH_4 dissociation on gold-alloyed Ni(111) is still unclear. Kratzer and his co-workers [11] only investigated the first step of CH_4 dissociation on gold-alloyed Ni(111). In addition, spin polarization was neglected in their calculation.

With recent developments, density functional theory (DFT) method has already been extensively used to provide qualitative and quantitative insights into the structure of active surface and surface reaction [13−17]. Nowadays, several theoretical studies of CH_x ($x = 1\sim4$) adsorption and dissociation on metal surface have been reported [18−24]. In our previous work, we have studied the dissociation of CH_4 on NiCo(111) surface, and the results show that C is easy to form on the surface by DFT method [25]. In this contribution, the first principle density functional theoretical investigation of the systematic mechanism of CH_4 dissociation on gold-alloyed Ni(111) surface were carried out, aimed at understanding the mechanism how carbon formation is suppressed. The adsorption geometries and energies of CH_4 sequence dehydrogenation products on the surface have been investigated. Based on

* Corresponding author. Tel: +86-351-6018539; Fax: +86-351-6041237; E-mail: wangbaojun@tyut.edu.cn

The work was supported financially by the National Basic Research Program of China (No. 2005CB221203), the National Natural Science Foundation of China (No. 20976115) and the National Younger Natural Science Foundation of China (No. 20906066).

doi:10.1016/S1003-9953(10)60252-6

the optimized adsorption geometries, the decomposition of CH_4 was investigated, and then the results have been compared with those obtained on pure Ni(111) surface. Finally, the electronic properties of the surfaces have been plotted to explain the properties of adsorption and activation.

2. Computational details

2.1. Computational method

Density functional theory (DFT) calculations were performed using the Cambridge Sequential Total Energy Package (CASTEP) [26,27]. All calculations were conducted with the generalized gradient approximation (GGA) using Perdew-Burke-Ernzerhof (PBE) exchange correlation functional [28]. Ionic cores were described by ultrasoft pseudopotential [29] and the Kohn-Sham one-electron states were expanded in a plane-wave basis set up to a cutoff of 340 eV. A Fermi smearing of 0.1 eV was utilized and the corrected energy extrapolated to zero Kelvin. Brillouin zone integration was approximated by a sum over special k-points chosen using Monkhorst-Pack method [30], and they were set up to $5\times5\times1$. Geometries were optimized until the energy had converged to 2.0×10^{-5} eV/atom and the force converged to 0.005 eV/ nm and the max displacement converged to 0.2×10^{-3} nm. Spin polarization was considered in all calculations.

2.2. Surface models

Gold atoms alloyed into Ni surface offer an ideal system to study the effect of alloying on the chemical reactivity of a catalyst. Zhang et al. [31,32] detected the most simple Ni(111) by X-ray diffraction (XRD) technique. Therefore, we focused the reaction mechanism on the most regular (111) surface. The surfaces were obtained by cutting bulk Ni with a face-centered cubic structure along [111] direction. The thickness of each surface slab was chosen to be at least as thick as a three-layer Ni(111) slab, which is proved reasonable to investigate the adsorption and reaction mechanism in literature [25,33−35]. A (2×2) supercell was used in the calculation in order to reduce the interaction between adsorbed molecules. One of the four Ni atoms in the unit cell of the topmost layer was replaced with gold, corresponding to a gold coverage of 1/4 ML. The vacuum region between adjacent slabs was in excess of 1 nm. In order to decrease the computational load, the bottom layer of slab was fixed at its equilibrium bulk phase position, with a lattice constant of 0.3500 nm, while the top two layers and the adsorbates were allowed to relax freely.

The chemisorption energies, E_{ads}, were calculated, as follows:

$$E_{ads} = E_{adsorbates/slab} - (E_{adsorbates} + E_{slab})$$

where, $E_{adsorbates/slab}$ is the total energy of adsorbates on gold-alloyed Ni(111), $E_{adsorbates}$ is the total energy of isolated adsorbates which was calculated by putting the isolated adsorbates in a cubic box of $1\times1\times1$ nm^3, E_{slab} is the total energy of gold-alloyed Ni(111) slab.

The reaction energy was calculated by two different definitions given as follows:

$$\Delta E_s = [E_{A/slab} + E_{B/slab}] - [E_{AB/slab} + E_{slab}]$$

$$\Delta E_c = E_{A+B/slab} - E_{AB/slab}$$

where, $E_{A/slab}$, $E_{B/slab}$ and $E_{AB/slab}$ are the total energies of adsorbates A, B and AB adsorption on gold-alloyed Ni(111) surface, respectively, E_{slab} is the total energy of gold-alloyed Ni(111) slab, $E_{A+B/slab}$ is the total energy of the coadsorbed A and B on gold-alloyed Ni(111) surface. For reaction AB→ A+B, positive value suggests endothermic, while negative value suggests exothermic.

3. Results and discussion

3.1. Surface properties

Calculated structural parameters of pure and gold-alloyed Ni(111) surfaces are collected in Table 1. On gold-alloyed Ni(111) surface, Ni atoms of the first layer (Ni^1) move inward (into the bulk) while Au^1 atoms relax outward (to the surface) with respect to the computed Ni bulk-terminated geometry. The vertical displacement Δz is larger for Ni^1 than for Au^1 atoms: the values for gold-alloyed Ni(111) surface are 0.0041 and 0.0475 nm, respectively. Opposite displacements of the atoms cause a notable surface corrugation. Thus, the layer spacing is obviously increased for gold-alloyed Ni(111) than that for pure Ni(111), namely, addition of Au changes the geometry structure of Ni(111) surface, even changes the catalytic activity of the surface. This is consistent with the results from STM study [10].

Table 1. Vertical atomic displacements (Δz, nm) for pure and gold-alloyed Ni(111) surfaces

	$\Delta z(Ni^1)^*$	$\Delta z(Ni^2)$	$\Delta z(Au^1)$	d_{12}^{Ni}	d_{12}^{AuNi}
On pure Ni(111)	0.0035	0.0038		0.2475	
On gold-alloyed Ni(111)	0.0041	0.0035	−0.0475	0.2459	0.2899

* Ni^1 (Au^1) and Ni^2 denote Ni (Au) atoms of the first and second layers, respectively. Δz refers to the atomic displacement perpendicular to the surface. Negative Δz denotes an outward displacement, toward the vacuum, positive Δz denotes an atom movement in the direction of the bulk

3.2. CH_4 dissociation

CH_x ($x = 1\sim3$) preferable occupying threefold sites have been proved by experimental observations and theoretical calculations [18−25,36,37]. Herein, we only examine CH_x ($x = 0\sim3$) and H species adsorbed at the highly coordinated threefold hollow sites. These adsorption sites are presented in Figure 1. It is clear that each group of the threefold site is split into two subsets.

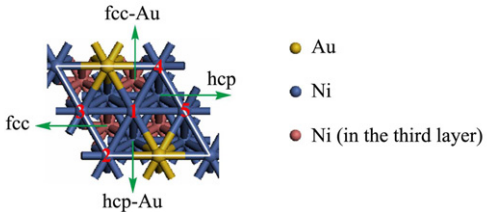

Figure 1. Surface and adsorption sites of gold-alloyed Ni(111)

3.2.1. $CH_4 \rightarrow CH_3+H$

Adsorption of CH_4, CH_3 and H: The adsorption of methane molecule on transition metal surfaces is generally classified as a process of physisorption where the attractive interaction arises from the van der Waals force. Previous calculation results have proved that the adsorption energy of CH_4 is substantially small on transition metal surface, which may be negligible [38,39]. Hence only one kind of geometry of CH_4 adsorption is considered on gold-alloyed Ni(111) surface, that is, three H atoms point to the surface, another H points to the surface normal, as shown in Figure 2(a). The calculated adsorption energy is −0.01 eV, in accord with previous calculated results [40] and experimental observations [41,42].

For CH_3 adsorption, C−H bond points toward the nearest-neighbor metal atoms, and the distances of C−H both are elongated to about 0.1113 nm at fcc and hcp sites. Our calculated adsorption energy of CH_3 at fcc site (shown in Figure 2b) is −1.45 eV, which is more stable than that (−1.40 eV)

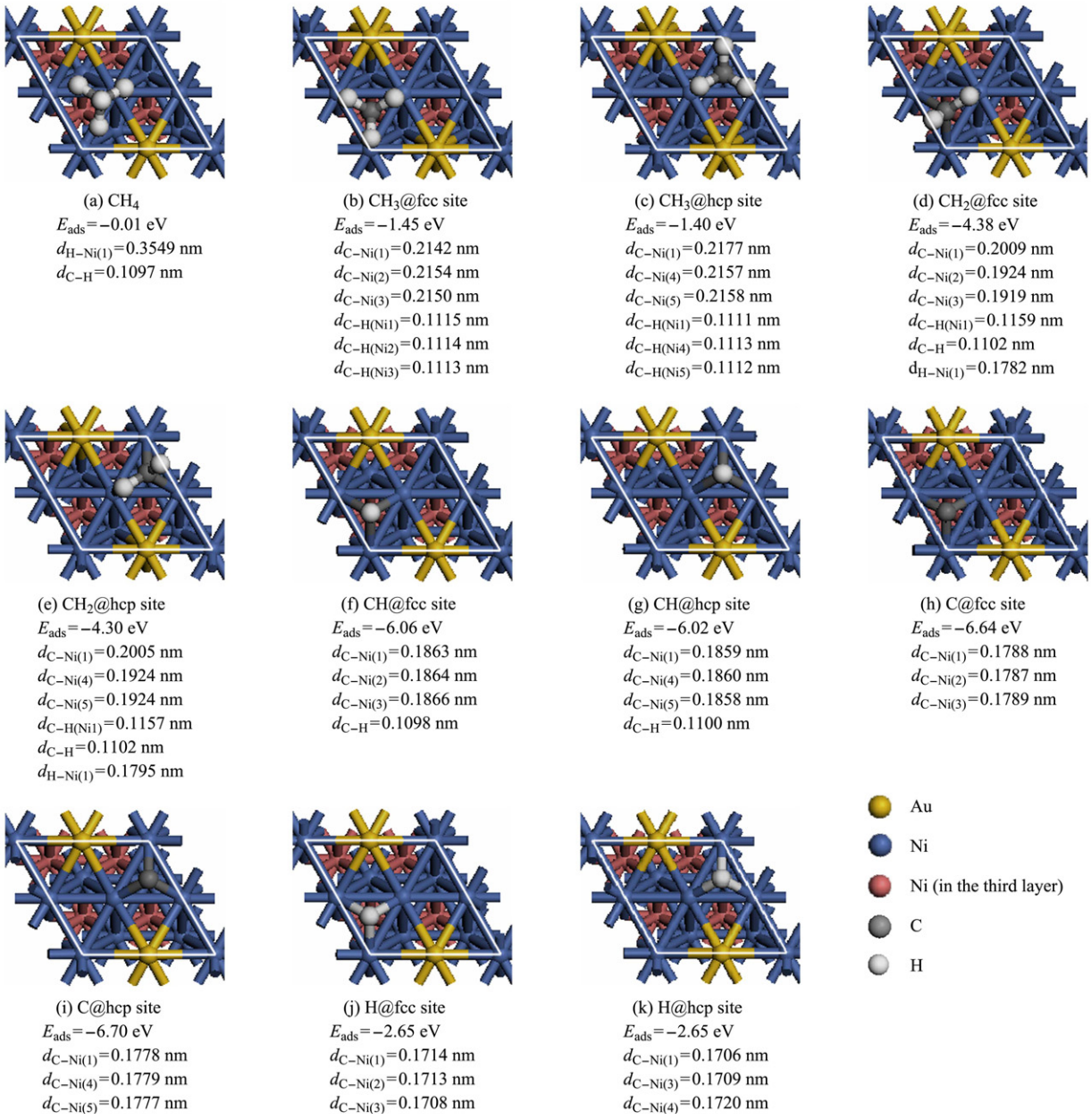

Figure 2. Adsorption geometries and parameters of CH_x ($x = 0 \sim 4$) and H on gold-alloyed Ni(111)

at hcp site (shown in Figure 2c). It is interesting to note that the initial structures for CH_3 adsorbed on fcc-Au and hcp-Au sites were optimized into fcc and hcp sites, respectively, indicating the substitution of Ni surface atoms with Au atoms blocks active sites partly, even those in the neighbor of Au atoms. This result is in agreement with that obtained by Kratzer et al. [11]. Therefore, we do not consider the adsorption geometries on fcc-Au and hcp-Au sites in the following study.

Our calculated adsorption energies for CH_3 are -1.78 eV on hcp site and -1.81 eV on fcc site on pure Ni(111), and the longest distance of C−H is 0.1115 nm in configuration of CH_3 adsorbed on fcc site. Compared with CH_3 adsorption on pure Ni(111), the adsorption energies are lower and the distance of C−H is slightly shorter on corresponding sites on gold-alloyed Ni(111), which indicates that substituting Ni surface atoms with Au decreases the adsorption energy of CH_3.

For H adsorption, they have the equal adsorption energies of -2.65 eV at fcc and hcp sites (shown in Figures 2j and 2k). However, on pure Ni (111), the adsorption energies of H are -2.74 eV on hcp site and -2.77 eV on fcc site, respectively, which are higher than those on corresponding sites on gold-alloyed Ni(111).

Coadsorption of CH_3 and H: In order to investigate CH_4 sequence dehydrogenation on gold-alloyed Ni(111) surface, firstly it is necessary to investigate the coadsorption of CH_x($x = 0\sim3$) and H. Because the preferred site of CH_3 is at fcc site, only one coadsorption mode, namely, CH_x($x = 0\sim3$) is considered to preadsorb at fcc site while H coadsorbs at hcp site in a linear way.

To elucidate the lateral interaction arising from coadsorption species, it is necessary to value the difference (ΔE_{ads}) in adsorption energies between coadsorption species [$E_{ads}(CH_x/H)$], with respect to CH_x and H, and the sum of CH_x and H individual adsorptions on the same site as in coadsorption [$E_{ads}(CH_x) + E_{ads}(H)$]. The positive energy differences indicate that there are repulsive interactions between the adsorbed CH_x and H.

The coadsorption energies and calculated bond parameters for CH_3 and H are present in Figure 3. The coadsorption energy of CH_3 and H is -3.83 eV. ΔE_{ads} is 0.27 eV, indicating slight repulsion interactions in CH_3 and H coadsorption geometries. The coadsorption configuration is considered as the final state (FS) of the first step in CH_4 dissociation on gold-alloyed Ni(111).

TS of $CH_4 \rightarrow CH_3$+H: Based on physisorbed CH_4 and coadsorbed CH_3 and H, CH_4 dissociation is examined first, and the possible path is mapped out, as shown in Table 2. The geometry and parameters of the possible transition state are present in Figure 4. CH_4 dissociates on top of a Ni atom into CH_3 and H via TS1 along with CH_3 moving to fcc site and H moving to the opposite hcp site. The reaction needs to overcome the energy barrier of 1.77 eV. In the transition state TS1, the breaking C−H bond is elongated to 0.1712 nm, and the forming H−Ni bond is 0.1461 nm and C−Ni bond is 0.2201 nm. This reaction is endothermic by 0.60 eV (ΔE_S). Our calculated reaction barrier is 1.18 eV on pure Ni (111) [43], which is higher by 0.59 eV than that on gold-alloyed Ni(111). However, Kratzer et al. [11,12] obtained that the difference of reaction barriers in the first step of CH_4 dissociation on gold-alloyed Ni(111) and pure Ni(111) is 0.39 eV, lower than our result. The difference may be caused by used models and calculation methods mentioned in the introduction.

Table 2. Reaction barriers and reaction energies of successive dehydrogenation of CH_4 on gold-alloyed Ni(111) and pure Ni(111) (in parentheses)

Paths for dissociation of CH_4		Reaction barrier (E_a, eV)	Reaction energy (ΔE_c, eV)	Reaction energy (ΔE_s, eV)
$CH_4 \rightarrow CH_3$+H	Physisorbed $CH_4 \rightarrow$ TS1-1 $\rightarrow CH_3$+H	1.77(1.18)	0.87(0.39)	0.60(0.13)
$CH_3 \rightarrow CH_2$+H	fcc $CH_3 \rightarrow$ TS2-1 $\rightarrow CH_2$+H	0.79(0.78)	0.23(0.21)	0.15(0.11)
$CH_2 \rightarrow$ CH+H	fcc $CH_2 \rightarrow$ TS3-1 $\rightarrow$ CH+H	0.35(0.37)	−0.37(−0.34)	−0.34(−0.24)
CH → C+H	fcc CH→ TS4-1→ C+H	1.56(1.36)	0.81(0.61)	0.75(0.59)

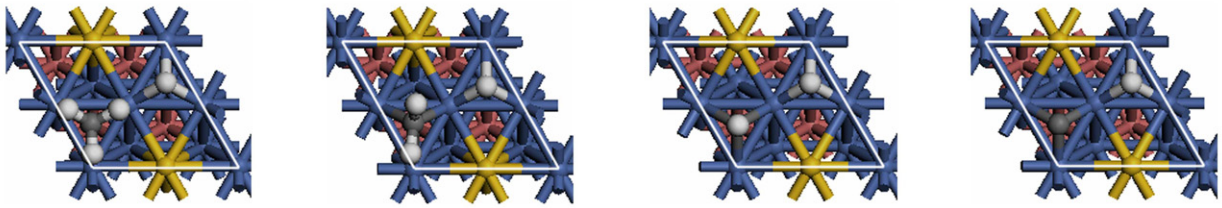

CH_3/H
E_{ads}=−3.83 eV
ΔE_{ads}=0.27 eV
$d_{C-Ni(1)}$=0.2290 nm
$d_{C-Ni(2)}$=0.2305 nm
$d_{C-Ni(3)}$=0.2089 nm
$d_{C-H(Ni1)}$=0.1107 nm
$d_{C-H(Ni2)}$=0.1105 nm
$d_{C-H(Ni3)}$=0.1102 nm
$d_{H-Ni(1)}$=0.1694 nm
$d_{H-Ni(4)}$=0.1686 nm
$d_{H-Ni(5)}$=0.1652 nm

CH_2/H
E_{ads}=−6.95 eV
ΔE_{ads}=0.08 eV
$d_{C-Ni(1)}$=0.1923 nm
$d_{C-Ni(2)}$=0.2057 nm
$d_{C-Ni(3)}$=0.1913 nm
$d_{C-H(Ni2)}$=0.1100 nm
d_{C-H}=0.1144 nm
$d_{H-Ni(1)}$=0.1685 nm
$d_{H-Ni(4)}$=0.1711 nm
$d_{H-Ni(5)}$=0.1667 nm

CH/H
E_{ads}=−8.74 eV
ΔE_{ads}=−0.03 eV
$d_{C-Ni(1)}$=0.1862 nm
$d_{C-Ni(2)}$=0.1863 nm
$d_{C-Ni(3)}$=0.1867 nm
d_{C-H}=0.1096 nm
$d_{H-Ni(1)}$=0.1702 nm
$d_{H-Ni(4)}$=0.1700 nm
$d_{H-Ni(5)}$=0.1714 nm

C/H
E_{ads}=−9.23 eV
ΔE_{ads}=0.06 eV
$d_{C-Ni(1)}$=0.1788 nm
$d_{C-Ni(2)}$=0.1787 nm
$d_{C-Ni(3)}$=0.1788 nm
$d_{H-Ni(1)}$=0.1688 nm
$d_{H-Ni(4)}$=0.1687 nm
$d_{H-Ni(5)}$=0.1688 nm

Figure 3. Optimized geometries of coadsorbed CH_x ($x = 0\sim3$) and H on gold-alloyed Ni(111)

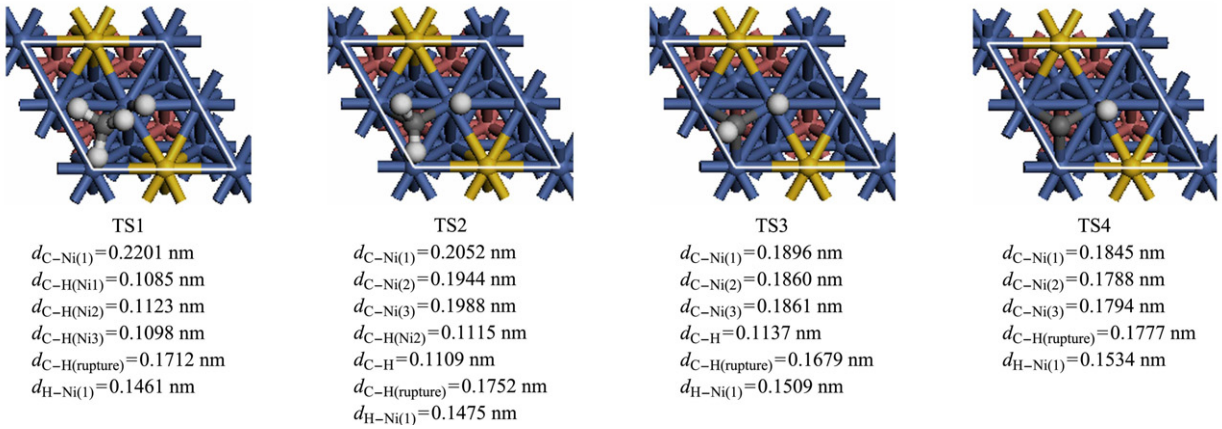

Figure 4. Optimized structures of the transition states of CH_4 sequence dissociation on gold-alloyed Ni(111)

3.2.2. $CH_3 \rightarrow CH_2+H$

Adsorption of CH_2: The adsorbed CH_2 has two types of inequivalent C−H bonds (shown in Figures 2d and 2e): one H points toward the Ni atom, the other H points toward the midway of the Ni–Ni bridge site, resulting in different activation characteristics of the two C−H bonds. For example, when CH_2 adsorbs at fcc or hcp site, one C−H bond in which H points toward Ni atom is stretched to about 0.1785 nm, and another C−H bond is 0.1102 nm. The calculated adsorption energies of CH_2 are −4.38 eV at fcc site and −4.30 eV at hcp site on gold-alloyed Ni(111). Our calculated bond lengths of C−H are 0.1165 nm, 0.1103 nm on fcc site and 0.1157 nm, 0.1102 nm on hcp site, respectively, and the calculated adsorption energies of CH_2 are −4.67 eV on fcc site and −4.65 eV at hcp site on pure Ni(111). Clearly, the adsorption of CH_2 is lower after inserting Au atom on pure Ni(111) surface.

Coadsorption of CH_2 and H: The coadsorption of CH_2 and H is examined. As shown in Figure 3, the coadsorption energy is −6.95 eV, and ΔE_{ads} in the coadsorption mode is 0.08 eV, indicating a slight repulsive interaction between CH_2 and H.

TS of $CH_3 \rightarrow CH_2$+H: Considering the most stable CH_3 adsorbed at fcc site as the initial state (IS) and coadsorbed configuration of CH_2 and H as the FS, the transition state of CH_3 dissociation is searched. Similar to the path of CH_4 dissociation into CH_3 and H, a possible path is designed for CH_3 dehydrogenation. The geometry and parameters of the possible transition state are present in Figure 4. CH_3 dissociates into CH_2 and H via TS2 along with H moving to the opposite hcp site. The energy barrier is 0.79 eV, which is approximate to that (0.78 eV) on pure Ni(111) [43], and it is kinetically favorable compared with the first dehydrogenation step. In the transition state TS2, the distance of breaking C−H bond is stretched to 0.1752 nm, and the forming bond length of H−Ni is shortened to 0.1475 nm. This reaction is found to be endothermic by 0.15 eV (ΔE_s).

3.2.3. $CH_2 \rightarrow CH+H$

Adsorption of CH: CH is absorbed at fcc site with the remaining H atom oriented perpendicular to the surface, as shown in Figures 2(f) and 2(g). The adsorption energies are −6.02 eV and −6.06 eV at hcp and fcc sites on gold-alloyed Ni(111), respectively, while they are −6.24 eV and −6.15 eV at hcp and fcc sites on pure Ni (111), respectively. Clearly, it is easy to conclude that addition of Au on pure Ni(111) surface decreases the adsorption energy of CH.

Coadsorption of CH and H: The coadsorption geometry for CH and H is shown in Figure 3. The coadsorption energy is −8.74 eV. The lateral interaction between CH and H in the coadsorption mode is −0.03 eV, which indicates slight attractive interaction between CH and H. The coadsorption configuration is selected as the FS for CH dehydrogenation reaction.

TS of $CH_2 \rightarrow$ CH+H: According to the configurations of CH_2 at fcc site and FS, the possible reaction path is conceived for CH_2 dehydrogenation. The geometry and parameters of the possible transition states are present in Figure 4. In the transition state TS3, the rupturing C−H bond is increased to 0.1679 nm, the forming H−Ni bond is shortened to 0.1509 nm. This reaction is exothermic by 0.34 eV [ΔE_s] and needs to overcome a lowest energy barrier of 0.35 eV, approximately equal to that (0.37 eV) on pure Ni(111) [43].

3.2.4. $CH \rightarrow C+H$

Adsorption of C: For C adsorption, the preferred binding site is at hcp site with the adsorption energy of −6.70 eV (shown in Figure 2i). At fcc site, the adsorption energy of C is −6.64 eV. Our calculated adsorption energies of C on pure Ni(111) are −6.90 eV at hcp site and −6.80 eV at fcc site, which are higher than those on corresponding adsorption sites on gold-alloyed Ni(111), indicating that addition of Au reduces the adsorption energy of C. This finding of the adsorption properties of Ni changed significantly after the ad-

dition of Au, which is consistent with the experimental observation of the suppression of H_2 and N_2O chemisorption by Chin et al [44].

Coadsorption of C and H As shown in Figure 3, the coadsorption of C and H has slight repulsive interaction compared with the sum of individual adsorption energies. Thus, coadsorption configuration is considered as the FS for the reaction of CH dehydrogenation.

TS of CH→ C+H: Similar to the above steps of CH_x dissociation, the possible path is designed for CH dehydrogenation. The geometry and parameters of the possible transition state are present in Figure 4. In the transition state TS4, the breaking C−H bond is elongated to 0.1777 nm, and the forming H−Ni bond is 0.1534 nm. The reaction barrier and the reaction energy are 1.56 and 0.75 eV (ΔE_s), respectively. On pure Ni(111), the reaction barrier is 1.36 eV [43], which is lower than that on gold-alloyed Ni(111).

3.3. Energetics of dissociation CH_4

According to reaction barriers (E_a) and reaction energies (ΔE_c and ΔE_s) of the successive dehydrogenation of CH_4 on gold-alloyed Ni(111) and pure Ni(111), we plot the optimal potential energy surfaces, as displayed in Figure 5. For each dehydrogenation step, the initial state is taken as a $CH_x(x = 1\sim4)$ species, the final state is $CH_{x-1}(x = 1\sim4)$ species plus one coadsorbed H atom at the same unit cell and adsorbed (4-x)H atoms at infinite distance at stable fcc site [$CH_{x-1}(x = 1\sim4)$/H, and $CH_{x-1}(x = 1\sim4)$+(4-x)H]. The energy of $CH_{x-1}(x = 1\sim4)$ plus (4-x) H atoms at infinite distance [$CH_{x-1}(x = 1\sim4)$+(4-x)H] is considered to be the starting point for the following step.

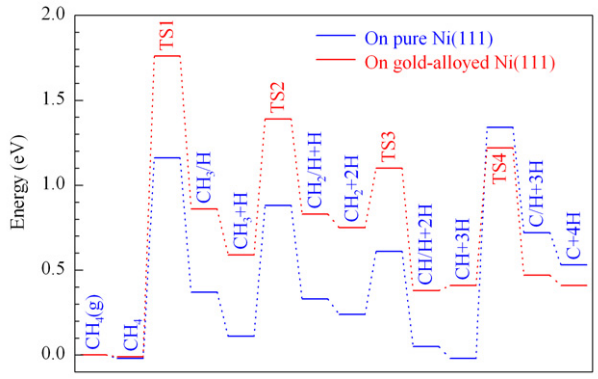

Figure 5. Potential energy surface of CH_4 dissociation on pure Ni (111) and gold-alloyed Ni(111). CH_x/H($x = 0\sim3$) denotes the co-adsorbed CH_x and H, CH_x+H denotes the adsorbed CH_x and H separately, CH_4 (g) denotes the free CH_4 molecule, respectively

From Figure 5, the activation energy of TS1 is found to be the highest on gold-alloyed Ni(111), so one can conclude that the first step of CH_4 dissociation into CH_3 and H is the rate-determining step in the reaction of CH_4 dissociation on gold-alloyed Ni(111). However, it is clear that the rate-determining step is the reaction of CH dissociation on pure Ni(111). Furthermore, the reaction barrier in rate-determining step for CH_4 dissociation is higher by 0.41 eV than that on pure Ni(111). Therefore, one can conclude that substituting surface atoms with Au can resist carbon formation. This result is consistent with the results obtained by Kratzer et al [11,12] and Chin et al. [44]. Chin and co-workers [44] found that adding Au to Ni catalysts reduced both the amount of formed carbon and the rate of carbon deposition.

3.4. Electronic properties

In order to gain an insight into the physical origin of the difference in catalytic activity, electronic property analysis is necessary. The d-band center describing the electronic effect of the surface is calculated by the formula [11]:

$$\varepsilon_d^c = \frac{\int_{-\infty}^{E_f} E\rho_d(E)dE}{\int_{-\infty}^{E_f} \rho_d(E)dE}$$

where, ρ_d represents the density of state projected onto the surface d-band, and E_f is the Fermi energy.

The projected densities of states (PDOS) onto the surface d-band (shown in Figure 6) are calculated and d-band centers are −1.87 eV and −2.33 eV for pure and gold-alloyed Ni(111) surface, respectively. It is lower by 0.46 eV on gold-alloyed Ni(111) relative to the pure Ni(111) surface, which is in line with literatures [11,12]. In general, the closer the d-band center to the Fermi level is, the more reactive the surface is. Obviously, d-band center of gold-alloy Ni(111) surface is farther away from the Fermi level than that of pure Ni(111). Therefore, it is less reactive than pure Ni(111) surface. This is consistent with our above calculated results: adsorption energies decrease and reaction barriers increase on gold-alloyed Ni(111) compared with those on pure Ni(111). Detailed analysis found that d-band center shift can well explain the reactivity variation of the surface in the presence of Au.

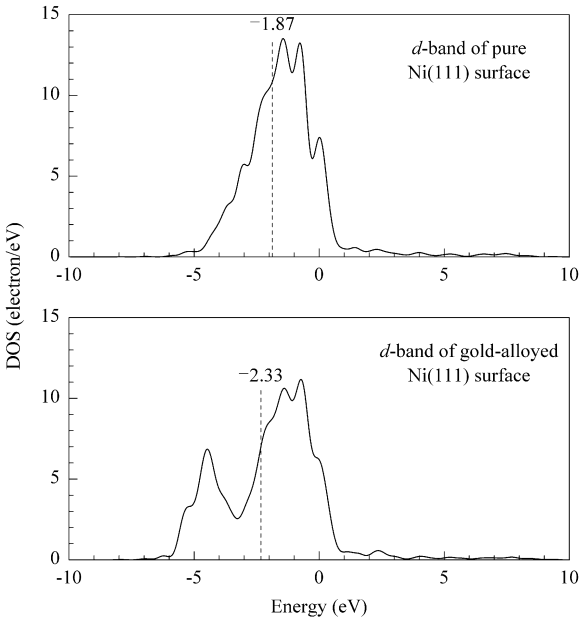

Figure 6. PDOS of pure Ni(111) and gold-alloyed Ni(111)

4. Conclusions

In this work, we conduct a DFT-based computational study on the adsorption and dissociation of CH_x on gold-alloyed Ni(111) surface, and compare the results with those on pure Ni(111). DFT calculations show that the preferred site on gold-alloyed Ni(111) is consistent with those on pure Ni(111). On the basis of the coadsorption of CH_x and H, the dissociation of CH_x($x = 1\sim4$) is investigated. The results show the activation energy in CH_4 dissociation is increased on gold-alloyed Ni(111) compared with that on pure Ni (111). The rate-determining step for CH_4 dissociation is considered as the first step of dehydrogenation on gold-alloyed Ni(111), while it is the fourth step of dehydrogenation on pure Ni(111). Especially, the reaction barrier of rate-determining step for CH_4 dissociation is higher by 0.41 eV on gold-alloyed Ni(111) than that on pure Ni(111). Therefore, one can believe that carbon is not easy to form on gold-alloyed Ni(111).

Acknowledgements

The work was supported financially by the National Basic Research Program of China (No. 2005CB221203), the National Natural Science Foundation of China (No. 20976115) and the National Younger Natural Science Foundation of China (No. 20906066).

References

[1] Tomishige K, Chen Y G, Fujimoto K. *J Catal*, 1999, 181(1): 91
[2] Rostrupnielsen J R, Hansen J H B. *J Catal*, 1993, 144(1): 38
[3] Erdohelyi A, Cserenyi J, Solymosi F. *J Catal*, 1993, 141(1) 287
[4] Tokunaga O, Osada Y, Ogasawara S. *Fuel*, 1989, 68 (8): 990
[5] Kim J H, Suh D J, Park T J, Kim K L. *Appl Catal A*, 2000, 197(2): 191
[6] Takahashi R, Sato S, Sodesawa T, Kato M, Takenaka S, Yoshida S. *J Catal*, 2001, 204(2): 259
[7] Tang S, Ji L, Lin J, Zeng H C, Tan K L, Li K. *J Catal*, 2000, 194(2): 424
[8] Sehested J. *Catal Today*, 2006, 111(1-2): 103
[9] Wei J M, Iglesia E. *J Catal*, 2004, 224(2): 370
[10] Nielsen L P, Besenbacher F, Stensgaard I, Legsgaard E, Engdahl C, Stoltze P, Jacobsen K W, Nørskov J K. *Phys Rev Lett*, 1993, 71(5): 754
[11] Kratzer P, Hammer B, Nørskov J K. *J Chem Phys*, 1996, 105(13): 5595
[12] Besenbacher F, Chorkendorff I, Clausen B S, Hammer B, Molenbroek A M, Nørskov J K, Stensgaard I. *Science*, 1998, 279(5358): 1913
[13] Nave S, Tiwari A K, Jackson B. *J Chem Phys*, 2010, 132(5): 054705
[14] Torres D, Lopez N, Illas F. *J Catal*, 2006, 243(2): 404
[15] Yang T, Wen X D, Huo C F, Li Y W, Wang J, Jiao H. *J Mol Catal A*, 2009, 302(1-2): 129
[16] Zhang R G, Liu H Y, Zheng H Y, Ling L X, Li Z, Wang B J. *Appl Surf Sci*, 2011, 257(11): 4787
[17] Zhang R G, Wang B J, Ling L X, Liu H Y, Huang W. *Appl Surf Sci*, 2010, 257(4): 1175
[18] Yang H, Whitten J L. *Surf Sci*, 1991, 255(1-2): 193
[19] Yang H, Whitten J L. *J Am Chem Soc*, 1991, 113(17): 6442
[20] Yang H, Whitten J L. *J Chem Phys*, 1992, 96(7): 5529
[21] Michaelides A, Hu P. *Surf Sci*, 1999, 437(3): 362
[22] Michaelides A, Hu P. *J Chem Phys*, 2000, 112(13): 6006
[23] Michaelides A, Hu P. *J Chem Phys*, 2000, 112(18): 8120
[24] Zuo Z J, Huang W, Han P D, Li Z H. *Appl Surf Sci*, 2010, 256(20): 5929
[25] Liu H Y, Zhang R G, Yan R X, Wang B J, Xie K C. *Appl Surf Sci*, 2011, 257(21): 8955
[26] Payne M C, Teter M P, Allan D C, Arias T A, Joannopoulos J D. *Rev Mod Phys*, 1992, 64(4): 1045
[27] Milman V, Winkler B, White J A, Pickard C J, Payne M C, Akhmatskaya E V, Nobes R H. *Int J Quantum Chem*, 2000, 77(5): 895
[28] Perdew J P, Burke K, Ernzerhof M. *Phys Rev Lett*, 1996, 77(18): 3865
[29] Vanderbilt D. *Phys Rev B*, 1990, 41(11): 7892
[30] Monkhorst H J, Pack J D. *Phys Rev B*, 1976, 13(12): 5188
[31] Zhang W, Ge Q J, Xu H Y. *Chin J Catal (Cuihua Xuebao)*, 2010, 31(9): 1162
[32] Zhang W, Ge Q J, Xu H Y. *Chin J Catal (Cuihua Xuebao)*, 2010, 31(11): 1358
[33] Shah V, Li T, Baumert K L, Cheng H S, Sholl D S. *Surf Sci*, 2003, 537(1-3): 217
[34] Wang S G, Cao D B, Li Y W, Wang J G, Jiao H J. *Surf Sci*, 2006, 600(16): 3226
[35] Liu H Y, Zhang R G, Ding F Y, Yan R X, Wang B J, Xie K C. *Appl Surf Sci*, 2011, 257(22): 9455
[36] Siegbahn P E M, Panas I. *Surf Sci*, 1990, 240(1-3): 37
[37] Swang O, Faegri Jr K, Gropen O, Wahlgren U, Siegbahn P. *Chem Phys*, 1991, 156(3): 379
[38] Moussounda P S, Haroun M F, M'Passi-Mabiala B, Légaré P. *Surf Sci*, 2005, 594(1-3): 231
[39] Sorescu D C. *Phys Rev B*, 2006, 73(15): 155420
[40] An W, Zeng X C, Turner C H. *J Chem Phys*, 2009, 131(17): 174702
[41] Lee M B, Yang Q Y, Ceyer S T. *J Chem Phys*, 1987, 87(5): 2724
[42] Lee M B, Yang Q Y, Tang S L, Ceyer S T. *J Chem Phys*, 1986, 85(3): 1693
[43] Liu H Y, Zhang R G, Yan R X, Wang B J, Xie K C. *Appl Surf Sci*, 2011, 257(21): 8955
[44] Chin Y H, King D L, Roh H S, Wang Y, Heald S M. *J Catal*, 2006, 244(2): 153